Direct Dynamics Trajectories Demonstrate Dynamic Matching and Nonstatistical Radical Pair Intermediates During Fe-Oxo Mediated C-H Functionalization Reactions

Jyothish Joy and Daniel H. Ess*

Department of Chemistry and Biochemistry, Brigham Young University, Provo, Utah 84602, United States

KEYWORDS. Direct dynamics, trajectories, nonstatistical, non-heme Fe-oxo, hydrogen atom transfer, C-H functionalization

Abstract

The generally proposed mechanism for the reaction between non-heme Fe-oxo complexes and alkane C-H bonds involves a hydrogen atom transfer reaction step with a radical pair intermediate that then has competitive radical rebound, dissociation, or desaturation pathways. Here we report density functional theory-based quasiclassical direct dynamics trajectories that examine post hydrogen atom transfer reaction dynamics. Trajectories revealed that the radical pair intermediate can be a nonstatistical type intermediate without complete internal vibrational redistribution and post hydrogen atom transfer selectivity is generally determined by dynamic effects. Fast rebound trajectories occur through dynamic matching between the rotational motion of the newly formed Fe-OH bond and collision with the alkane radical and all of this occurs through a nonsynchronous dynamically concerted process that circumvents the radical pair intermediate structure. For radical pair dissociation, trajectories proceeded to the radical pair intermediate for a very brief time followed by complete dissociation. These trajectories provide a new viewpoint and model to understand the inherent reaction pathway selectivity for non-heme Fe-oxo mediated C-H functionalization reactions.

Introduction

Heme and non-heme high-valent Fe-oxo complexes have the capability to functionalize strong, nonpolar sp³ C-H bonds. 1,2 Based on in-depth spectroscopic experiments and computational studies (density functional theory (DFT) and wavefunction), the general C-H functionalization mechanism involves a multistep process where the first step (generally rate limiting) is hydrogen atom transfer to the oxygen of the Fe-oxo to give a radical pair intermediate (Figure 1).3,4 From this radical pair intermediate there are then at least three possible diverging reaction pathways: i) radical rebound to form a hydroxylated product, 1,5,6 ii) the Fe-OH intermediate can induce a second hydrogen atom transfer to generate an alkene product, 7,9 and iii) dissociation of radical fragments. 10 These reaction pathways can occur on the same spin state surface as the first hydrogen atom transfer step or occur on a different spin state surface after spin crossover. 10 This second step is typically inferred to control regioselectivity and stereoselectivity. 3,4 For biomimetic model heme and non-heme Fe-oxo complexes, control of reaction pathway selectivity, regioselectivity, and stereoselectivity remains a major challenge, 4, 10-16 and therefore understanding fundamental control of the post hydrogen atom transfer reaction pathways can have a major impact on interpretation of experiments and design of new C-H functionalization catalysts.

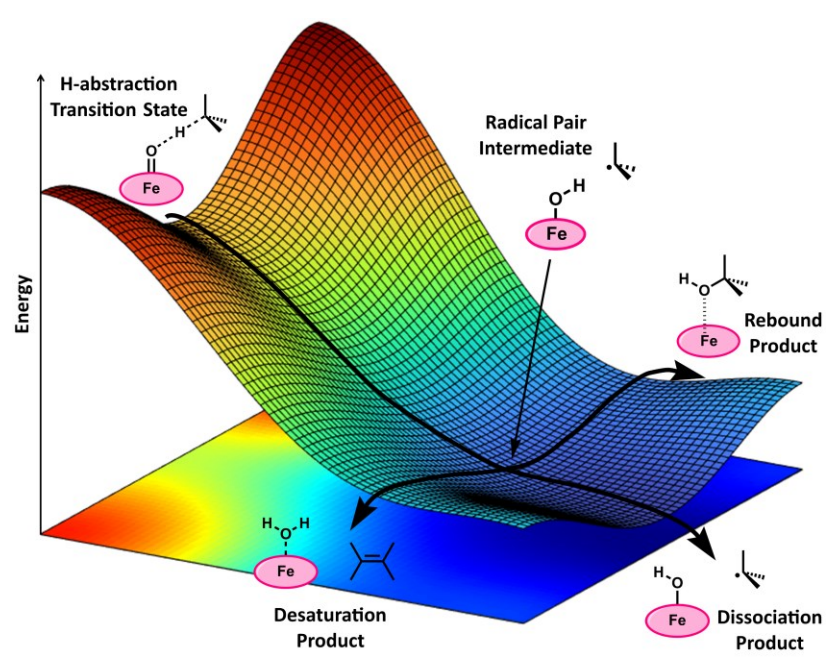


Figure 1. Graphical representation of a model potential energy landscape for Fe-oxo C-H hydroxylation of a sp³ C-H bond. The radical pair intermediate branches to either radical rebound, desaturation, or dissociation pathways.

Spectroscopic experiments and DFT calculations by Nam, Que, and Shaik^{10, 17} have showcased the importance of intermediates and spin states in controlling radical rebound versus dissociation pathways. For example, on one spin state surface there may be nearly barrierless radical rebound (e.g. a doublet spin state) whereas on another spin state there may be a very large barrier for radical rebound, which steers the reaction towards dissociation. ^{18, 19} Overall, this previous work focused on interpretation of pathway selectivity from a statistical transition-state theory perspective arising from the radical pair intermediate after hydrogen atom transfer. 10 More recently, Srnec and coworkers developed a kinetic energy distribution model for synthetic heme and non-heme Fe-oxo complexes to analyze reaction pathway preference based on the calculated transition-state structures for hydrogen atom transfer.²⁰ rather than the radical pair intermediate. This model emphasizes that significant localized kinetic energy of the transferring hydrogen atom facilitates a dissociation pathway while kinetic energy localized mostly on the radical substrate or on the Fe-oxo fragment facilitates rebound. From a similar perspective, a recent experimental and computational study by Sarkar and coworkers on methylcubane hydroxylation by cytochrome P450 implied the possibility of transition state motion influencing the reaction pathway after hydrogen atom transfer, and there was speculation about the possibility of dynamic effects, ²¹ but no dynamics trajectories were evaluated.

Our group has used quasiclassical direct dynamics to understand the reaction pathway selectivity for a variety of organometallic reactions.²² For example, we recently showed that the reaction of Cp(PMe₃)₂Re with ethylene requires reactive dynamics trajectories, rather than statistical transition state theory analysis, to model the reaction pathway selectivity between C-H insertion/oxidative addition versus π -coordination.²³ This was because the weak CH- σ -coordination complex that is a potential energy stationary point that precedes C-H insertion and π -coordination is in a very shallow potential energy well and trajectories revealed no pausing at this intermediate due to a lack of significant intramolecular (internal) vibrational energy redistribution (IVR).^{24, 25} We have previously called this type of intermediate with a very short lifetime due to the lack of complete IVR as a nonstatistical intermediate.^{22, 26} This previous discovery prompted us to use dynamics trajectories to determine if Fe-OH radical pairs formed from reaction between non-heme Fe-oxo complexes and alkanes that generally have a shallow potential energy well (Figure 1) are also nonstatistical intermediates. Previous DFT investigations on heme and non-heme iron-oxo complexes have shown that barriers for rebound and dissociation are relatively low and similar, ^{14, 20} which makes it challenging for statistical rate theories, such as transition state theory or RRKM theory, ^{27, 28} to accurately predict the product selectivity. The consequence of nonstatistical Fe-OH radical pair intermediates with a lack of complete IVR means that

the reaction pathway selectivity likely cannot be easily or fully determined by static DFT calculations, and reaction pathway branching could be due to dynamic effects rather than transition states.

Here we report DFT-based quasiclassical dynamics trajectories for the reactions between non-heme Fe-oxo complexes and cyclohexane that have been experimentally characterized to have either radical rebound or dissociation mechanisms. These trajectories revealed that in the radical rebound mechanism there is a nonsynchronous dynamically concerted pathway bypassing the radical pair intermediate. This bypassing is a case of post transition state dynamic matching between the rotational motion of the newly formed Fe-OH bond and collision with the cyclohexyl radical. For radical pair dissociation, trajectories proceeded to the radical pair intermediate, but only for a brief time, followed by complete dissociation. Overall, these trajectories provide a new viewpoint and model to understand the inherent reaction pathway selectivity (rebound and dissociation) for non-heme Fe-oxo mediated C-H functionalization reactions.

Computational Details

All structure optimizations were performed using UB3LYP-D3(BJ)/def2-SVP in Gaussian-16.²⁹⁻³³ This method and basis set combination has been extensively tested and performs well for the relative Fe-oxo spin state energies and barrier height.^{20, 34} Since the Fe-oxo complexes studied have either 1+ or 2+ overall charges, all structures were optimized using the CPCM solvation model for acetonirile.³⁵ Stationary points and transition states were characterized by frequency calculations.³³ Variational transition state optimizations showed extremely small geometry differences (see Supporting Information (SI) for a representative comparison). Quasiclassical direct dynamics trajectories were initialized and propagated (Verlet algorithm) using our program Milo, ³⁶ which interfaced with Gaussian 16 to evaluate energies and forces using UB3LYP-D3(BJ)/def2-SVP with an ultrafine integration grid and CPCM (acetonitrile) solvation. Trajectories were initiated at the hydrogen atom transfer transitionstate structure using local mode and thermal sampling that includes zero-point energy (ZPE) at the experimental temperatures (233.15K, 243.15K, 303.15K, and 233.15K respectively for complexes 1-4). Both forward and backward NVE trajectories were propagated with time step of 0.75 femtosecond (fs). The possibility of ZPE leakage effects were evaluated by running test calculations with 75% the ZPE contribution to the total kinetic energy.³⁷ Our test calculations showed that ZPE leakage has a negligible influence on the simulation results presented (see SI for details).

Results and Discussion

Fe-oxo complexes, transition states, and radical pair intermediates

Figure 2 shows complexes 1-4 that have been experimentally reported to have either rebound or dissociation pathway-based product selectivity. Complex 1, [(TQA_Cl)Fe^{IV}O]⁺, is a synthetic mimic of the halogenase enzyme that was demonstrated to catalyze cyclohexane functionalization with halogenation being the major product (~78%) and hydroxylation being the minor product (~15%).³⁸ Complex 2, [(PyTACN)Fe^{IV}(O)Cl]¹⁺, is also a model for non-heme iron halogenase and was shown not to yield halogenated products, either due to radical escape from the solvent cage through a dissociation pathway or due to hydroxide rebound.³⁹ Complex 3, [(N4Py)^{OMe,Me}Fe^{IV}O]²⁺, reaction with cyclohexane produced major amount of Fe^{III} complex (presumably the Fe-OH species and dissociated radicals; ~90%) and minor amount of iron(II) complex (rebound complex; ~10%).⁴⁰ Complex 4, [(PyNMe₃)Fe^VO(OAc)]²⁺, selectively hydroxylates unactivated C-H bonds with stereoretention in a site selective manner (cyclohexanol/cyclohexanone = 1/0.2).⁴¹ Based on these experiments, complexes 1-3 have preference for a dissociation pathway while complex 4 has selectivity for a radical rebound pathway.

Here cyclohexane was used as the sp³ C-H activation partner with reaction for complexes **1-4** because it is a general experimental substrate, and it minimizes the number of product pathways. Transition states and intermediates with complexes **1-3** have quintet spin state and complex **4** has a doublet spin state. These spin states are 5-10 kcal/mol lower in energy than the next lowest energy spin state. ^{20, 42}

Figure 2 shows 2D depictions of the high valent Fe-oxo complexes along with 3D depictions of the fully optimized hydrogen atom transfer transition states and their corresponding intermediate structures for the reactions examined here. Our optimized transition state and radical pair structures are in good agreement with those computed in several previous static DFT studies.^{20, 42, 43} As is typical in

many Fe-oxo sp³ C-H hydrogen atom transfer transition states, these transition states show only slightly elongated C-H bond distances and relatively advanced C-O bond forming distances. From these transition-state structures we performed intrinsic reaction coordinate (IRC) calculations⁴⁴ followed by geometry optimizations. On the potential-energy landscapes for complexes 1-3, the hydrogen atom transfer transition state connects to a radical pair intermediate structure (Figure 2). For complex 4, no stationary point structure for the radical pair intermediate was located.⁴² From a statistical model point of view, these energy landscapes suggest that for complexes 1-3 decent from the hydrogen atom transfer transition state should result in the radical pair intermediates and subsequent rebound versus dissociation pathway selectivity determined by transition states after the radical pair intermediates. For complex 4 the energy landscape suggests there should be exclusive formation of the rebound product. However, as mentioned in the introduction, previous calculations have shown that barriers for rebound and dissociation are relatively low (and often similar) which makes it very challenging for statistical rate theories to predict selectivity. This is also compounded by the difficulty of estimating the dissociation transition state energy on the Gibbs energy surface.

The concept of a radical pair intermediate during the C-H functionalization mechanism of alkanes by high valent Fe-oxo complexes has been supported by several experimental and computational studies. For example, the involvement of a radical pair intermediate is key to explain the radical probe experiments of Groves, 4,45 and the selectivity model proposed by Nam, Que, and Shaik. 10,10 However, there have also been experiments that suggest a highly fleeting nature of the radical pair intermediate to explain hypersensitive radical probe/clock experiments, especially those reported by Newcomb and coworkers 46-48 and Sarkar and coworkers. Thus, one of our major goals was to use dynamics trajectories to determine the post hydrogen-atom transfer evolution of the radical pair intermediate and its dynamical motion into product forming pathways.

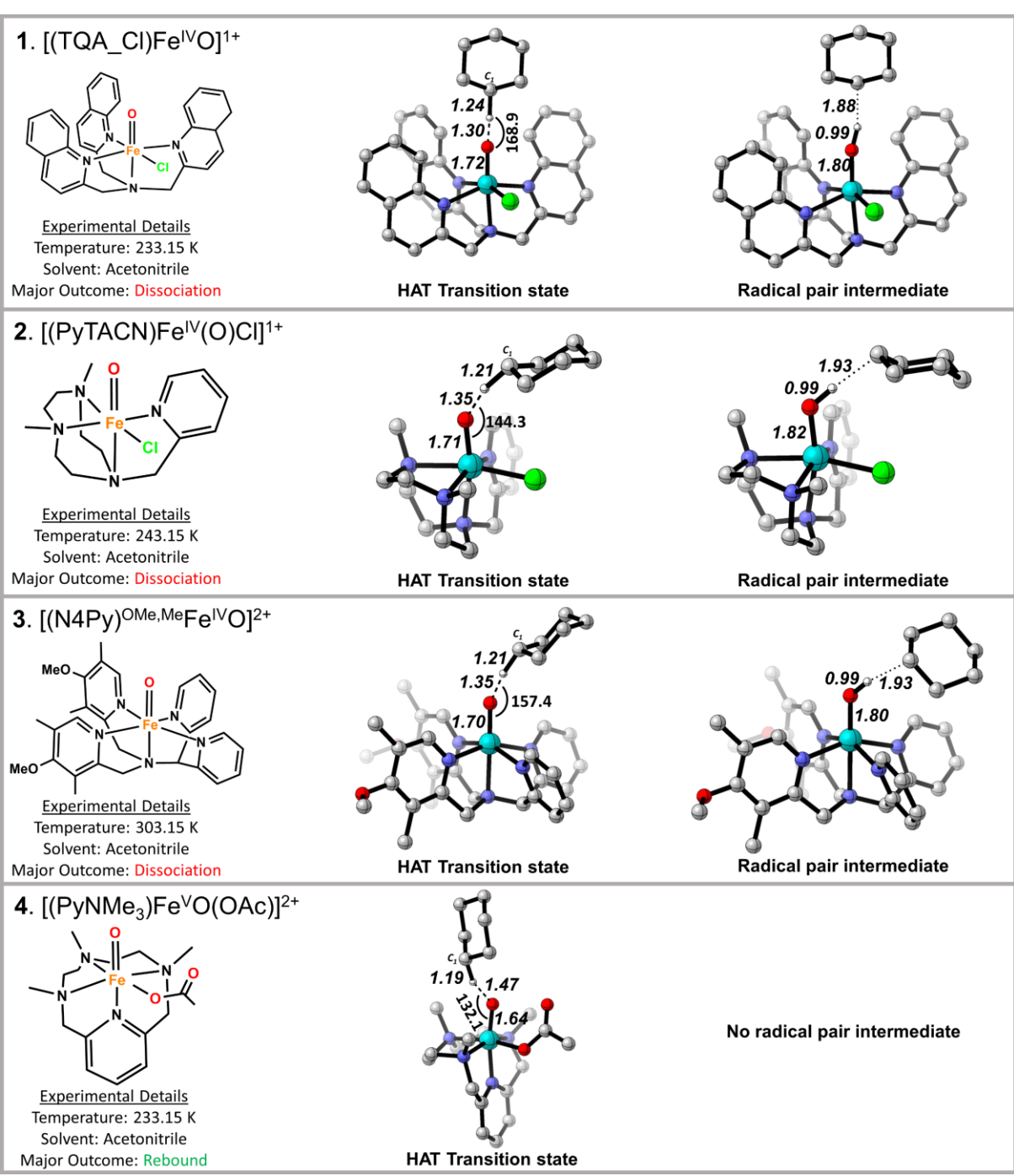


Figure 2. Fe-oxo complexes³⁸⁻⁴¹ examined with DFT-based direct dynamics trajectories. 3D rendering of the hydrogen atom transfer (HAT) transition-state structures and corresponding radical pair intermediates with key bond distances (Å) and angles (degree) calculated using UB3LYP-D3(BJ)/def2-SVP(acetonitrile continuum solvent).

Quasiclassical direct dynamics trajectories

For complexes 1-4, starting from the hydrogen atom transfer transition-state structures, 60 quasicalssical trajectories at the UB3LYP-D3(BJ)/def2-SVP(acetonitrile) level of theory were propagated both in the forward and backward directions. Trajectories were propagated along a single spin state (quintet for complexes 1-3 and doublet for complex 4) because test trajectories where we implemented Truhlar's two state spin mixed model⁴⁹ showed no significant spin mixing or spin crossover before product formation (see SI). There was only a small number of recrossing trajectories (13%, 5%, 2%, 2% respectively for complexes 1-4), which was expected based on the structure similarity between the optimized transitions-state structure and the variational transition-state structure,

as well as the steep slope on the potential energy surface. Figure 3 plots the cyclohexane C₁ to oxo oxygen atom distance (C–O distance) versus time for all forward direction trajectories. The transition state C–O distances have a range of 2.54-2.66 Å. At the end of 750 fs trajectories with a C–O distance >3.5 Å were classified as ending at dissociated radicals (gray lines), trajectories with a C–O distance between the transition-state structure distance and 3.5 Å were classified as ending at a radical pair intermediate (green lines), and trajectories with a C–O distance less than the transition-state structure distance were classified as rebound (red lines).

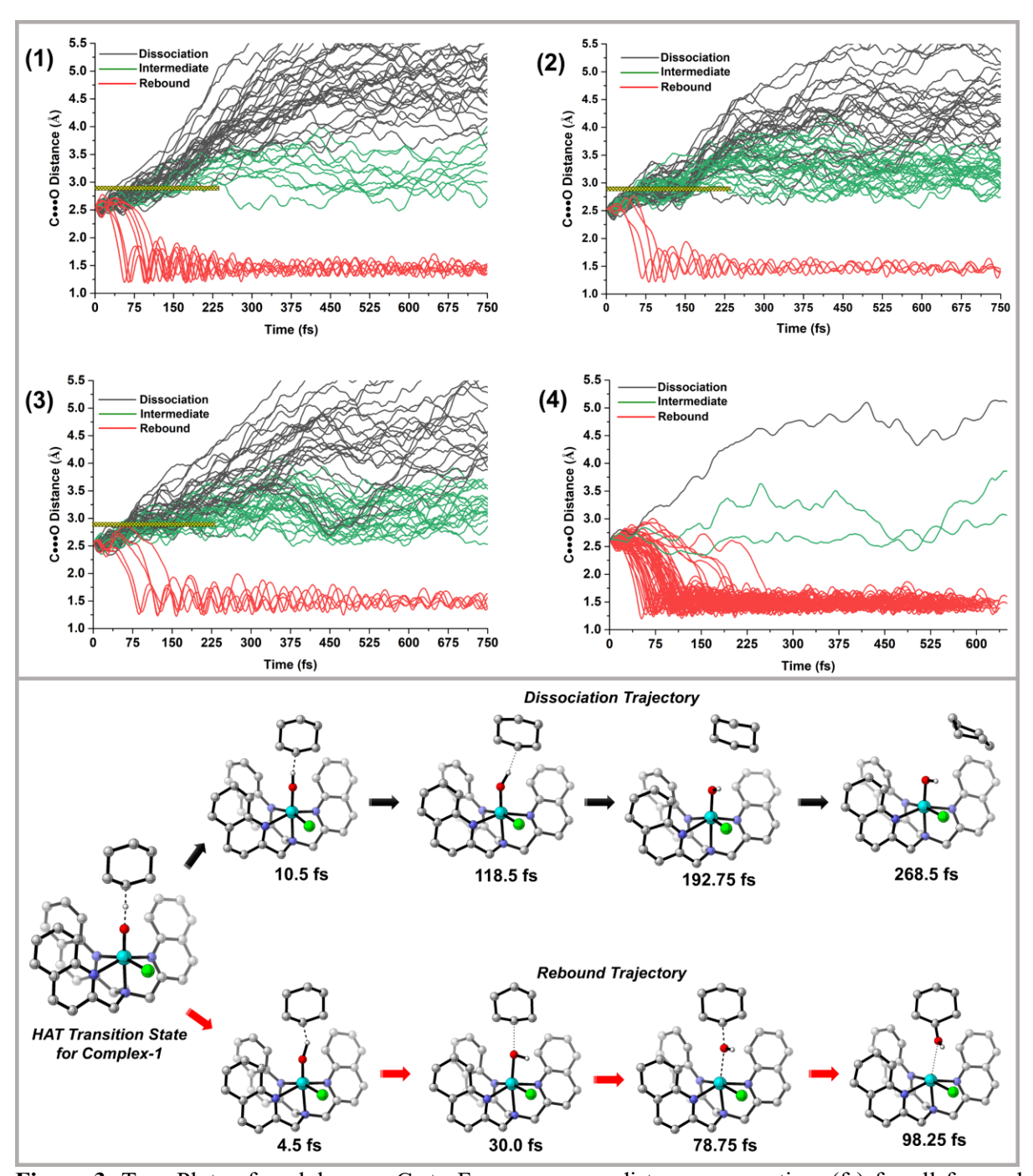


Figure 3. Top: Plots of cyclohexane C₁ to Fe-oxo oxygen distance versus time (fs) for all forward direction (breaking C–H bond) quasiclassical trajectories for complexes **1-4**. The transition state position is time zero. Gray colored lines are trajectories that end in radical pair dissociation. Green colored lines are trajectories that end in a radical pair intermediate. Red colored lines are trajectories that end in rebound. The horizontal yellow line represents the C-O distance for the optimized radical pair intermediate structure. Bottom: Snapshots of representative dissociation and rebound trajectories

for complex 1 starting from the hydrogen atom transfer (HAT) transition state. Most hydrogens on the cyclohexane and TQA (tris(2-quinolylmethyl)amine)) ligand are not shown for visual clarity.

Consistent with experiments, ³⁸⁻⁴⁰ our trajectory results for complexes 1 (66% dissociation, 14% rebound and 20% intermediate), 2 (48% dissociation, 7% rebound and 45% intermediate), and 3 (50% dissociation, 8% rebound and 42% intermediate), showed a major preference for the formation of either radical dissociation or radical pair intermediate. Surprisingly, but also consistent with experiments, there was up to 14% radical pair rebound. Trajectories for complex 4 showed a major preference for rebound (2% dissociation, 95% rebound and 3% intermediate), which again is in very good agreement with experimental results. ⁴¹ More interestingly, only a small portion of our trajectories followed the static DFT predicted mechanism (green lines) that involved a radical-pair type intermediate. Thus, in contrast to the potential-energy only DFT structures and landscapes, which only portrays a multistep mechanism for complexes 1-3, a large portion of trajectories starting from the hydrogen atom transfer transition state directly led to dissociation of the radicals (gray lines) or directly to rebound (red lines) without spending significant time at or near the radical pair intermediate region of the potential energy surface.

In nearly all trajectories the initial hydrogen atom transfer process is very fast and occurs within 10-20 fs from the transition-state structure time. On average, radical rebound occurs at 89 ± 26 fs for complex 1, 87 ± 18 fs for complex 2, 116 ± 29 fs for complex 3, and 104 ± 27 fs for complex 4. A reaction process is often considered concerted when the time gap between consecutive steps is less than 60 fs⁵⁰ (the approximate lifetime of a transition state with zero activation energy).^{51, 52} Based on this definition, all the rebound trajectories should probably best be considered nearly concerted (although nonsynchronous⁴⁷) and there is an extremely short time between hydrogen atom transfer and C-O bond formation. It is important to note that for all the complexes there is a set of trajectories with fast radical rebound occurs within 75 fs and there is another set of trajectories that take up to about 150 fs to rebound, which skews the average formation time of the C-O bond. This observation of extremely fast rebound trajectories and slightly slower rebound trajectories is in good agreement with Goldberg's kinetic measurements of a corrole-ligated Fe(OH) complex where both concerted and stepwise rebound pathways were observed.² These life-time measurements are also in the range of previous ab initio dynamic simulations of cytochrome P450 enzyme models^{53, 54} and Houk's dynamics simulations of radical oxygen rebound during the oxidation of isobutane by dimethyldioxirane.⁵⁵ Moreover, similar to the ideas proposed by Goldberg et al., Newcomb et al., 46 and Sarkar et al. 21 our trajectory results support the viewpoint that rebound is perhaps better considered a dynamically concerted process rather than a stepwise process.

A general assumption about the radical rebound mechanism, especially for Fe-oxo reactions, is that there is formation of the radical pair intermediate geometry prior to rebound motion, even if for only a brief time period of time. The horizontal yellow bar in Figure 3 (top panel) represents the DFT optimized C-O distance in the radical pair intermediate for complexes 1-3. Surprisingly, in all rebound trajectories (red lines), the hydroxyl group rebounds to the cyclohexane radical without attaining the radical pair intermediate structure. Also surprisingly, all dissociation trajectories (gray lines) formed a structure with the intermediate C-O distance, but only a small fraction of the trajectories remained at this distance for more than 200 fs. This indicates that for complexes 1-3 the radical pair intermediates are perhaps best described as nonstatistical intermediates that likely do not undergo complete internal vibrational redistribution (IVR) before entering the rebound or dissociation reaction stages. ^{24, 56, 57} This indicates that the post-transition state dynamics from the hydrogen atom transfer transition state controls rebound versus dissociation pathway selectivity and there is an effective dynamic bifurcation area. Shaik et al. previously envisioned this type of dynamic pathway selectivity as a possible alternative to the two-state reactivity paradigm.¹⁷ Importantly, this type of dynamic selectivity model is fundamentally different than a statistical model based on a radical pair intermediate that then has competitive transition states leading to either rebound or dissociation. Our trajectories showing an extremely short lifetime of the radical pair intermediate are consistent with the radical clock/probe experiments of Newcomb and coworkers who observed very fast rebound step in hydroxylations by P-450 enzymes ($k_{ox} = 1.4 \times 10^{10}$ to 1.4 x 10¹³ s⁻¹).⁴⁷ Lifetime measurements of their putative intermediates were found to be 80-200 fs, which is too short of a time for the formation of a radical pair intermediate. 46-⁴⁸ Overall, our trajectory results are consistent with the general description by Newcomb and coworkers

that radical pair intermediates can be considered as part of a reacting ensemble produced in a non-synchronous concerted process.⁴⁷

The dynamically concerted nature of the rebound trajectories, regardless of whether there is a radical pair intermediate on the potential energy surface, suggests that the hydrogen atom transfer and C-O bond formation reaction steps are dynamically coupled. To understand this reaction step coupling, Figure 4 shows More O'Ferrall-Jencks type plot for the evolution of the C-O bond as a function of the O-H bond distance starting from the hydrogen atom transfer transition state (cyan dot) all the way to the products through the radical pair intermediate structure (purple dot). Gray and red lines color code dissociation and rebound trajectories, respectively. These plots reveal that for all complexes, 1-4, red rebound trajectories never generate structures with the same partial bond distances as the radical pair intermediates (compare with yellow bar in Figure 3 top panel). This figure shows that after the C-H bond is broken and the O-H bond is formed, all rebound trajectories do not spend significant time in the region of 1.7 Å – 2.3 Å for the C–O bond distance, which is evidence of a fast radical recombination process. This suggests that the rebound trajectories entirely bypass the traditional two-step mechanism²⁵, ⁵⁸ and instead follow a new dynamical mechanism that directly leads from the hydrogen atom transfer transition state to the rebound product. This supports the speculations of Sarkar and coworkers and Srnec and coworkers that there is dynamic coupling between the hydrogen atom transfer and the rebound reaction steps.^{20, 21}

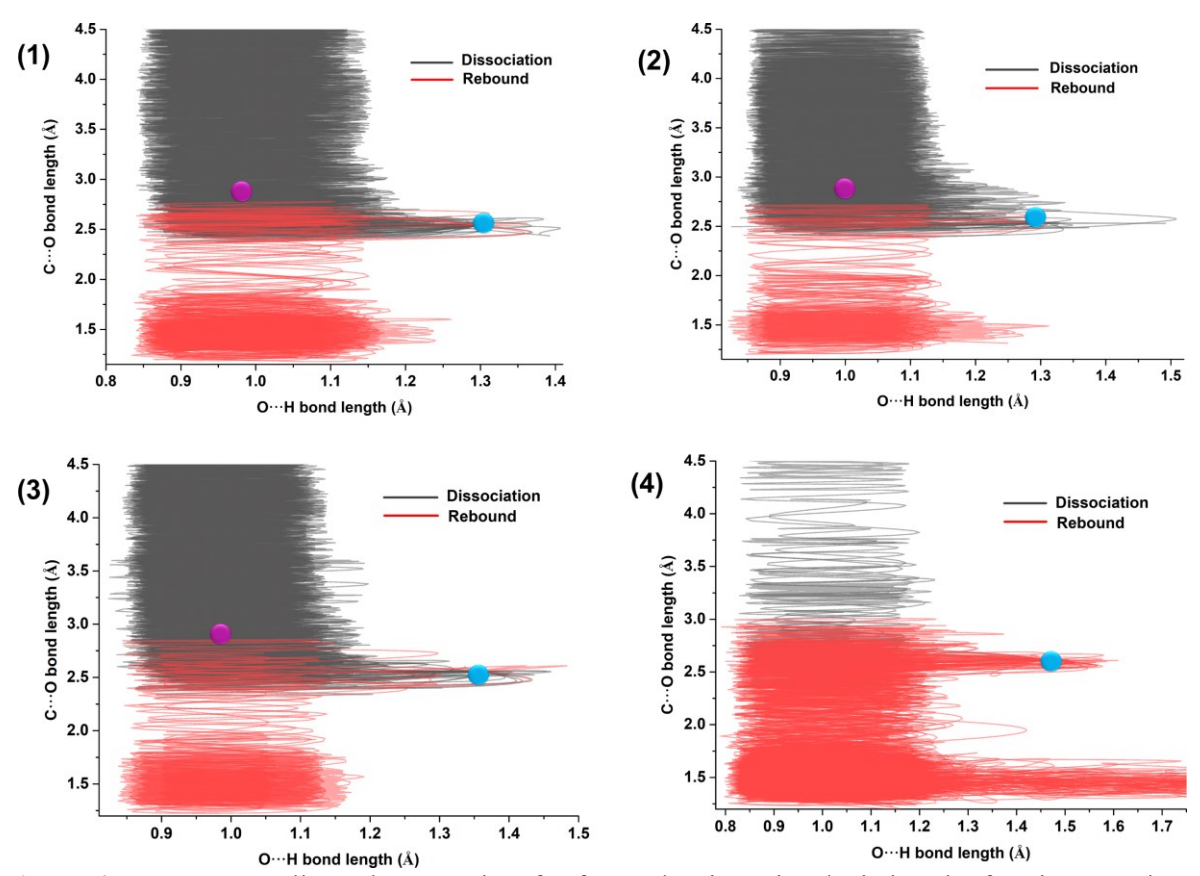


Figure 4. More O'Ferrall-Jencks type plots for forward trajectories depicting the forming O-H bond distance as a function of C-O bond distance for complexes **1–4**. Shortening and lengthening of the C-O bond typifies rebound (red lines) and dissociation (gray lines) trajectories respectively. Cyan dots indicate the hydrogen atom transfer transition state and purple dots indicate the radical pair intermediate structures. Here, all rebound trajectories bypassed the radical pair intermediate structure en route to rebound product pathway.

Dynamical matching during rebound trajectories

The concept of dynamic matching to explain pathway selectivity of nonstatistical dynamical reactions was pioneered by Carpenter. ^{59, 60} Doubleday, Houk, Singleton, Hase, Tantillo, and others have

also used trajectories to showcase dynamic matching effects in organic reactions. ⁶¹⁻⁶³ Generally, dynamic matching indicates that there is a geometric and atomic momentum correlation between the entry into a transition state and a post-transition state pathway that determines product selectivity. ⁶⁴ Often dynamic matching occurs in systems where there is incomplete IVR and a nonstatistical intermediate. ^{22, 25} Therefore, we wondered if the rebound trajectories in these non-heme Fe-oxo reactions are the result of dynamic matching, which can be anticipated from the experimental and static DFT results of methylcubane hydroxylation by cytochrome P450. ²¹ Related dynamics effects on the carbonylation versus epoxidation selectivity in alkene oxidation by a laboratory-evolved iron-heme P450 enzyme (anti-Markovnikov oxygenase - aMOx) was recently proposed by Hammer and Garcia-Borràs based on experiments and simulations. ⁶⁵

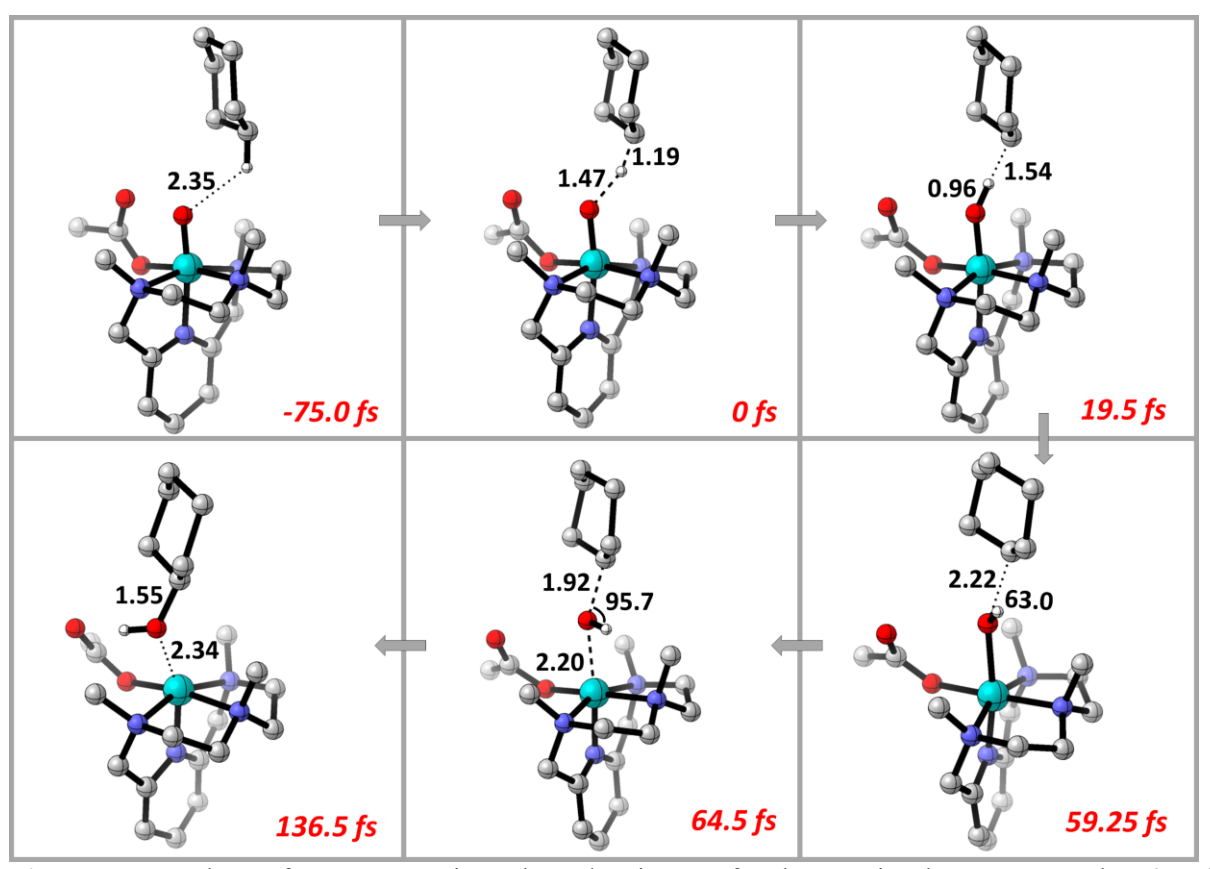


Figure 5. Snapshots of a representative rebound trajectory for the reaction between complex **4** and cyclohexane. Most hydrogens on the cyclohexane and PyNMe₃ ligand are not shown for visual clarity. 0 fs corresponds to the transition state geometry.

Because the rebound reaction mechanism between complex 4 and cyclohexane is a one-step process it should exemplify dynamic matching that occurs in reactions of high-valent Fe-oxo complexes with various alkanes. Figure 5 shows snapshots of a representative rebound trajectory for reaction of complex 4 with cyclohexane. The transition state is the 0 fs snapshot, and negative time is prior to the transition state and positive time is post transition state. The -75.0 fs snapshot represents the weakly bound reaction complex leading to the transition structure (0 fs). The 19.5 fs snapshot represents the putative radical-pair type structure formed immediately after the hydrogen transfer transition state, where the C–H bond is fully broken (1.54 Å), a new O–H bond is fully formed (0.96 Å), and the Fe(OH) group and the cyclohexane radical are in close proximity (2.50 Å). Despite this close proximity of radicals, rebound process does not begin until the newly formed O–H bond in the Fe(OH) group rotates away from the hydrocarbon radical to create a direct C···O contact (2.22 Å, 59.25 fs). Such short time gaps (~40 fs) are consistent with the velocities of simple bond stretches or rotations.⁵⁹ After this rotation, ^{53, 54} the C–O–H angle (63.0°) is in proper alignment for bonding overlap between the singly occupied orbitals in the Fe(OH) group and the cyclohexane radical, leading to the formation of the C–O bond via oxygen rebound (64.5 fs). By 136.5 fs the rebound product is fully formed. On the contrary,

for the dissociation trajectories, the putative radical pair like structure formed after the transition state does not undergo fast reorientation with the newly formed FeO–H bond, which prevents the coupling between the radicals leading to the dissociation product (cf. Figure 3 bottom panel).

Figure 6 plots the C-O-H angle (the angle formed between the cyclohexane radical carbon and the newly formed O-H bond) versus the C-O bond distance (either forming or dissociating) for trajectories of complexes 1-4. Red and gray lines represent rebound and dissociation trajectories respectively. Here, rebound trajectories are typified by a larger change in C-O-H angle and shortening of the C-O bond. Whereas dissociation trajectories show a smaller C-O-H angle and the eventual lengthening of the C-O bond. For rebound trajectories, after hydrogen atom transfer is complete, the C-O-H angle requires an increase to more than 90° to enable bonding overlap between radical pairs before collapsing into the rebound product. Importantly, all rebound trajectories quickly achieve this angle change without significant change in the C-O bond distance. This indicates that the dynamics of the C-O-H angle change is the key entry gate for radical recombination in the rebound mechanism. Thus, our findings correct the 'side-on' H-abstraction proposed by Newcomb and coworkers for the rebound mechanism (having short lifetime radicals), ⁴⁷ and show that conventional linear C-O-H abstraction followed by reorientation of the Fe(OH) group is the operating mechanism of nonsynchronous concerted rebound reactions. For most of the dissociation trajectories, the C-O-H angle is typically < 90° before the radicals begin to separate (C-O distance > 3.5 Å) and this lack of angle change prevent rebound. Overall, these trajectories showcase that the angle of incidence of the cyclohexane C-H bond and the ease of reorientation in the Fe(OH) group has major impact on the rebound product selectivity. For example, the angle of incidence in the transition state for complex 4 is 132.1° (see Figure 2), which makes minimal geometrical reorganization for both the Fe(OH) fragment and cyclohexane fragment to enter into the rebound product forming pathway. While more reactions need to be examined with trajectories, this initial work suggests that future designs of new Fe-oxo complexes with significant rebound can be achieved by minimizing this Fe-oxo to C-H bond angle.

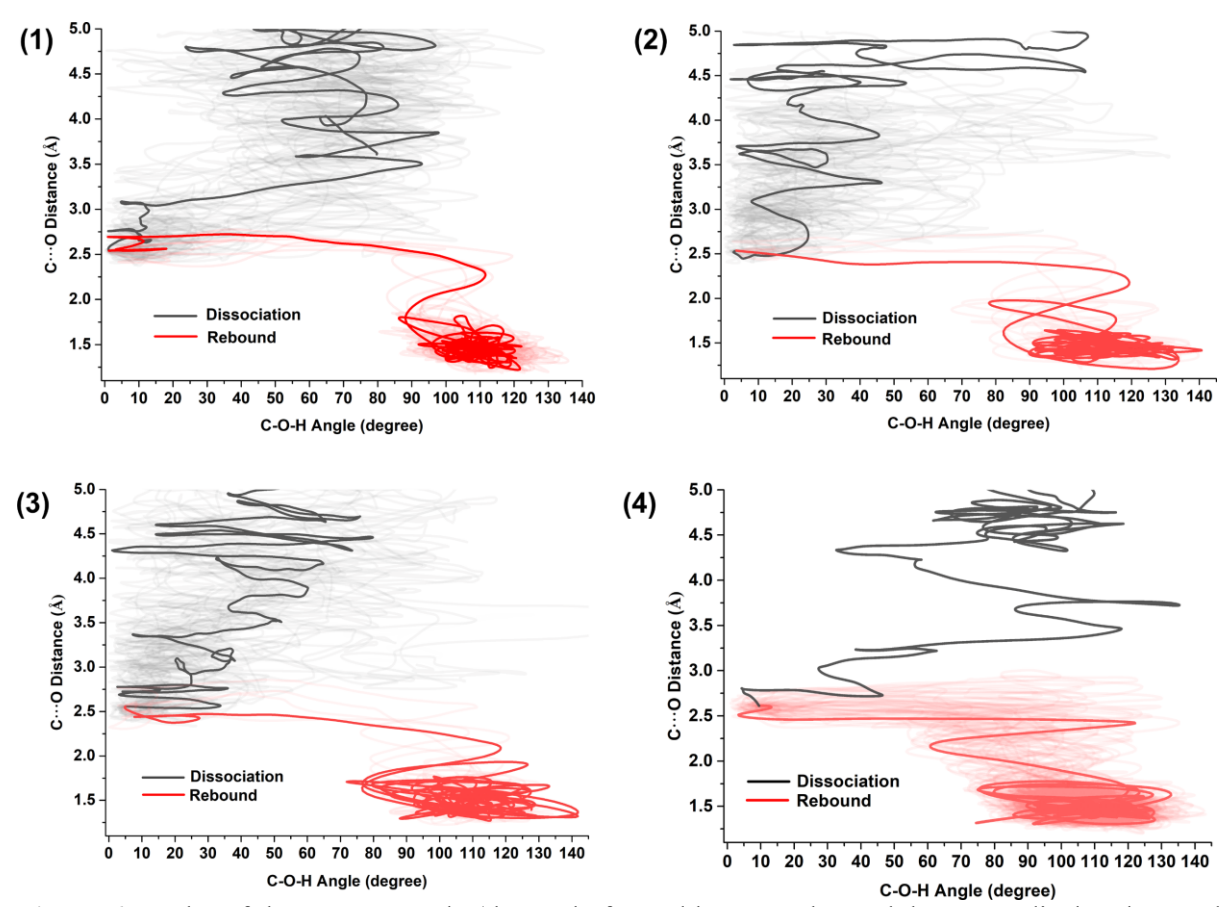


Figure 6. A plot of the C–O–H angle (the angle formed between the cyclohexane radical carbon and the newly formed O–H bond) versus the C–O bond distance for complexes **1-4**. Red and gray lines represent rebound and dissociation trajectories respectively.

Conclusions

The reaction between non-heme Fe-oxo complexes and alkanes is generally proposed to occur through a hydrogen atom transfer reaction step that results in a radical pair intermediate that then has competitive radical rebound, dissociation, or desaturation pathways. DFT-based quasiclassical direct dynamics trajectories were used to examine reaction dynamics that occur after hydrogen atom transfer for four experimentally reported non-heme Fe-oxo complexes with cyclohexane. Trajectories revealed that dynamic effects control post-hydrogen atom transfer pathway selectivity for rebound versus dissociation and that the radical pair intermediate is probably best described as nonstatistical. Rebound trajectories occur through dynamic matching between the rotational motion of the newly formed Fe-OH bond and collision with the cyclohexyl radical and all of this occurs through a nonsynchronous dynamically concerted process that circumvents the radical pair intermediate structure. For radical pair dissociation, trajectories proceeded to the radical pair intermediate for a very brief time period followed by complete dissociation. Therefore, the origin of regioselectivity and stereoselectivity in radical rebound reactions is heavily influenced by dynamic matching and bypassing of radical pair intermediates. Moreover, caution must be exercised when interpreting rebound versus dissociation selectivity based only on static DFT calculations. Future selectivity predictions should include dynamics trajectories. Overall, these trajectories provide a new viewpoint and model to understand the inherent reaction pathway selectivity (rebound and dissociation) for non-heme Fe-oxo mediated C-H functionalization reactions.

Acknowledgements

We thank Brigham Young University and the Fulton Supercomputing Lab for computational resources. We thank Michael Davenport for helping with mixed spin trajectory calculations. D.H.E. acknowledges the United States National Science Foundation Chemical Structure, Dynamics, and Mechanisms B (CSDM-B) Program under awards CHE 1952420 and CHE 2244799.

Notes

The authors declare no competing financial interest.

Supporting Information

Additional computational details, summary of reaction barriers, mixed spin trajectory calculations, variational transition states, examination of zero-point energy leakage, and cartesian coordinates of the complexes.

Corresponding Author

*dhe@chem.byu.edu

References

- (1) Ortiz de Montellano, P. R. Hydrocarbon Hydroxylation by Cytochrome P450 Enzymes. *Chem. Rev.* **2010**, *110*, 932-948
- (2) Zaragoza, J. P. T.; Yosca, T. H.; Siegler, M. A.; Moënne-Loccoz, P.; Green, M. T.; Goldberg, D. P. Direct Observation of Oxygen Rebound with an Iron-Hydroxide Complex. *J. Am. Chem. Soc.* **2017**, *139*, 13640-13643
- (3) Shaik, S.; Cohen, S.; Wang, Y.; Chen, H.; Kumar, D.; Thiel, W. P450 Enzymes: Their Structure, Reactivity, and Selectivity—Modeled by QM/MM Calculations. *Chem. Rev.* **2010**, *110*, 949-1017
- (4) Huang, X.; Groves, J. T. Beyond ferryl-mediated hydroxylation: 40 years of the rebound mechanism and C–H activation. *J. Biol. Inorg. Chem.* **2017**, *22*, 185-207
- (5) Groves, J. T.; McClusky, G. A. Aliphatic hydroxylation via oxygen rebound. Oxygen transfer catalyzed by iron. *J. Am. Chem. Soc.* **1976**, *98*, 859-861
- (6) Kovaleva, E. G.; Lipscomb, J. D. Versatility of biological non-heme Fe(II) centers in oxygen activation reactions. *Nat. Chem. Biol.* **2008**, *4*, 186-193
- (7) Grant, J. L.; Mitchell, M. E.; Makris, T. M. Catalytic strategy for carbon–carbon bond scission by the cytochrome P450 OleT. *Proc. Natl. Acad. Sci. U. S. A.* **2016**, *113*, 10049-10054
- (8) Rettie, A. E.; Rettenmeier, A. W.; Howald, W. N.; Baillie, T. A. Cytochrome P-450—Catalyzed Formation of Δ^4 -VPA, a Toxic Metabolite of Valproic Acid. *Science* **1987**, *235*, 890-893

- (9) Drummond, M. J.; Ford, C. L.; Gray, D. L.; Popescu, C. V.; Fout, A. R. Radical Rebound Hydroxylation Versus H-Atom Transfer in Non-Heme Iron(III)-Hydroxo Complexes: Reactivity and Structural Differentiation. *J. Am. Chem. Soc.* **2019**, *141*, 6639-6650
- (10) Cho, K.-B.; Hirao, H.; Shaik, S.; Nam, W. To rebound or dissociate? This is the mechanistic question in C–H hydroxylation by heme and nonheme metal–oxo complexes. *Chem. Soc. Rev.* **2016**, *45*, 1197-1210
- (11) Nam, W.; Lee, Y.-M.; Fukuzumi, S. Tuning Reactivity and Mechanism in Oxidation Reactions by Mononuclear Nonheme Iron(IV)-Oxo Complexes. *Acc. Chem. Res.* **2014**, *47*, 1146-1154
- (12) Wu, X.; Seo, M. S.; Davis, K. M.; Lee, Y.-M.; Chen, J.; Cho, K.-B.; Pushkar, Y. N.; Nam, W. A Highly Reactive Mononuclear Non-Heme Manganese(IV)—Oxo Complex That Can Activate the Strong C–H Bonds of Alkanes. *J. Am. Chem. Soc.* **2011**, *133*, 20088-20091
- (13) Cho, K.-B.; Shaik, S.; Nam, W. Theoretical Investigations into C–H Bond Activation Reaction by Nonheme Mn^{IV}O Complexes: Multistate Reactivity with No Oxygen Rebound. *J. Phys. Chem. Lett.* **2012**, *3*, 2851-2856
- (14) Cho, K.-B.; Wu, X.; Lee, Y.-M.; Kwon, Y. H.; Shaik, S.; Nam, W. Evidence for an Alternative to the Oxygen Rebound Mechanism in C–H Bond Activation by Non-Heme Fe^{IV}O Complexes. *J. Am. Chem. Soc.* **2012**, *134*, 20222-20225
- (15) Cho, K.-B.; Kang, H.; Woo, J.; Park, Y. J.; Seo, M. S.; Cho, J.; Nam, W. Mechanistic Insights into the C–H Bond Activation of Hydrocarbons by Chromium(IV) Oxo and Chromium(III) Superoxo Complexes. *Inorg. Chem.* **2014**, *53*, 645-652
- (16) Dhuri, S. N.; Cho, K.-B.; Lee, Y.-M.; Shin, S. Y.; Kim, J. H.; Mandal, D.; Shaik, S.; Nam, W. Interplay of Experiment and Theory in Elucidating Mechanisms of Oxidation Reactions by a Nonheme Ru^{IV}O Complex. *J. Am. Chem. Soc.* **2015**, *137*, 8623-8632
- (17) Shaik, S.; Cohen, S.; de Visser, Samuël P.; Sharma, Pankaz K.; Kumar, D.; Kozuch, S.; Ogliaro, F.; Danovich, D. The "Rebound Controversy": An Overview and Theoretical Modeling of the Rebound Step in C-H Hydroxylation by Cytochrome P450. *Eur. J. Inorg. Chem.* **2004**, 2004, 207-226
- (18) Ogliaro, F.; Harris, N.; Cohen, S.; Filatov, M.; de Visser, S. P.; Shaik, S. A Model "Rebound" Mechanism of Hydroxylation by Cytochrome P450: Stepwise and Effectively Concerted Pathways, and Their Reactivity Patterns. *J. Am. Chem. Soc.* **2000**, *122*, 8977-8989
- (19) Kumar, D.; de Visser, S. P.; Sharma, P. K.; Cohen, S.; Shaik, S. Radical Clock Substrates, Their C–H Hydroxylation Mechanism by Cytochrome P450, and Other Reactivity Patterns: What Does Theory Reveal about the Clocks' Behavior? *J. Am. Chem. Soc.* **2004**, *126*, 1907-1920
- (20) Maldonado-Domínguez, M.; Srnec, M. Understanding and Predicting Post H-Atom Abstraction Selectivity through Reactive Mode Composition Factor Analysis. *J. Am. Chem. Soc.* **2020**, *142*, 3947-3958
- (21) Sarkar, M. R.; Houston, S. D.; Savage, G. P.; Williams, C. M.; Krenske, E. H.; Bell, S. G.; De Voss, J. J. Rearrangement-Free Hydroxylation of Methylcubanes by a Cytochrome P450: The Case for Dynamical Coupling of C–H Abstraction and Rebound. *J. Am. Chem. Soc.* **2019**, *141*, 19688-19699
- (22) Ess, D. H. Quasiclassical Direct Dynamics Trajectory Simulations of Organometallic Reactions. *Acc. Chem. Res.* **2021**, *54*, 4410-4422
- (23) Yang, B.; Schouten, A.; Ess, D. H. Direct Dynamics Trajectories Reveal Nonstatistical Coordination Intermediates and Demonstrate that σ and π -Coordination Are Not Required for Rhenium(I)-Mediated Ethylene C–H Activation. *J. Am. Chem. Soc.* **2021**, *143*, 8367-8374
- (24) Carpenter, B. K. Energy Disposition in Reactive Intermediates. *Chem. Rev.* **2013**, *113*, 7265-7286 (25) Sun, L.; Song, K.; Hase, W. L. A S_N2 Reaction That Avoids Its Deep Potential Energy Minimum. *Science* **2002**, *296*, 875-878
- (26) Ma, X.; Hase, W. L. Perspective: chemical dynamics simulations of non-statistical reaction dynamics. *Philosophical Transactions of the Royal Society A: Mathematical, Physical and Engineering Sciences* **2017**, *375*, 20160204
- (27) Eyring, H. The Activated Complex in Chemical Reactions. J. Chem. Phys. 1935, 3, 107-115
- (28) Truhlar, D. G.; Garrett, B. C.; Klippenstein, S. J. Current Status of Transition-State Theory. *J. Phys. Chem.* **1996**, *100*, 12771-12800
- (29) Frisch, M. J.; Trucks, G. W.; Schlegel, H. B.; Scuseria, G. E.; Robb, M. A.; Cheeseman, J. R.; Scalmani, G.; Barone, V.; Petersson, G. A.; Nakatsuji, H.; Li, X.; Caricato, M.; Marenich, A. V.; Bloino, J.; Janesko, B. G.; Gomperts, R.; Mennucci, B.; Hratchian, H. P.; Ortiz, J. V.; Izmaylov, A. F.;

- Sonnenberg, J. L.; Williams-Young, D.; Ding, F.; Lipparini, F.; Egidi, F.; Goings, J.; Peng, B.; Petrone, A.; Henderson, T.; Ranasinghe, D.; Zakrzewski, V. G.; Gao, J.; Rega, N.; Zheng, G.; Liang, W.; Hada, M.; Ehara, M.; Toyota, K.; Fukuda, R.; Hasegawa, J.; Ishida, M.; Nakajima, T.; Honda, Y.; Kitao, O.; Nakai, H.; Vreven, T.; Throssell, K.; Montgomery, J. A., Jr.; Peralta, J. E.; Ogliaro, F.; Bearpark, M. J.; Heyd, J. J.; Brothers, E. N.; Kudin, K. N.; Staroverov, V. N.; Keith, T. A.; Kobayashi, R.; Normand, J.; Raghavachari, K.; Rendell, A. P.; Burant, J. C.; Iyengar, S. S.; Tomasi, J.; Cossi, M.; Millam, J. M.; Klene, M.; Adamo, C.; Cammi, R.; Ochterski, J. W.; Martin, R. L.; Morokuma, K.; Farkas, O.; Foresman, J. B.; Fox, D. J. Gaussian 16, Revision B.01; Gaussian Inc., Wallingford CT, 2016.
- (30) Becke, A. D. Density-functional thermochemistry. III. The role of exact exchange. *J. Chem. Phys.* **1993**, *98*, 5648-5652
- (31) Lee, C.; Yang, W.; Parr, R. G. Development of the Colle-Salvetti correlation-energy formula into a functional of the electron density. *Phys. Rev. B.* **1988**, *37*, 785-789
- (32) Grimme, S.; Ehrlich, S.; Goerigk, L. Effect of the damping function in dispersion corrected density functional theory. *J. Comput. Chem.* **2011**, *32*, 1456-1465
- (33) Weigend, F.; Ahlrichs, R. Balanced basis sets of split valence, triple zeta valence and quadruple zeta valence quality for H to Rn: Design and assessment of accuracy. *Phys. Chem. Chem. Phys.* **2005**, 7, 3297-3305
- (34) Altun, A.; Breidung, J.; Neese, F.; Thiel, W. Correlated Ab Initio and Density Functional Studies on H₂ Activation by FeO⁺. *J. Chem. Theory Comput.* **2014**, *10*, 3807-3820
- (35) Cossi, M.; Rega, N.; Scalmani, G.; Barone, V. Energies, structures, and electronic properties of molecules in solution with the C-PCM solvation model. *J. Comput. Chem.* **2003**, *24*, 669-681
- (36) Teynor, M. S.; Wohlgemuth, N.; Carlson, L.; Huang, J.; Pugh, S. L.; Grant, B. O.; Hamilton, R. S.; Carlsen, R.; Ess, D. H. *Milo, Revision 1.1.0*; Brigham Young University, Provo UT, 2022.
- (37) Doubleday, C.; Boguslav, M.; Howell, C.; Korotkin, S. D.; Shaked, D. Trajectory Calculations for Bergman Cyclization Predict H/D Kinetic Isotope Effects Due to Nonstatistical Dynamics in the Product. J. Am. Chem. Soc. 2016, 138, 7476-7479
- (38) Puri, M.; Biswas, A. N.; Fan, R.; Guo, Y.; Que, L. Modeling Non-Heme Iron Halogenases: High-Spin Oxoiron(IV)—Halide Complexes That Halogenate C—H Bonds. *J. Am. Chem. Soc.* **2016**, *138*, 2484-2487
- (39) Planas, O.; Clémancey, M.; Latour, J.-M.; Company, A.; Costas, M. Structural modeling of iron halogenases: synthesis and reactivity of halide-iron(IV)-oxo compounds. *Chem. Commun.* **2014**, *50*, 10887-10890
- (40) Rana, S.; Dey, A.; Maiti, D. Mechanistic elucidation of C–H oxidation by electron rich non-heme iron(IV)–oxo at room temperature. *Chem. Commun.* **2015**, *51*, 14469-14472
- (41) Serrano-Plana, J.; Oloo, W. N.; Acosta-Rueda, L.; Meier, K. K.; Verdejo, B.; García-España, E.; Basallote, M. G.; Münck, E.; Que, L., Jr.; Company, A.; Costas, M. Trapping a Highly Reactive Nonheme Iron Intermediate That Oxygenates Strong C—H Bonds with Stereoretention. *J. Am. Chem. Soc.* **2015**, *137*, 15833-15842
- (42) Mondal, B.; Neese, F.; Bill, E.; Ye, S. Electronic Structure Contributions of Non-Heme Oxo-Iron(V) Complexes to the Reactivity. *J. Am. Chem. Soc.* **2018**, *140*, 9531-9544
- (43) Terencio, T.; Andris, E.; Gamba, I.; Srnec, M.; Costas, M.; Roithová, J. Chemoselectivity in the Oxidation of Cycloalkenes with a Non-Heme Iron(IV)-Oxo-Chloride Complex: Epoxidation vs. Hydroxylation Selectivity. *J. Am. Soc. Mass Spectrom.* **2019**, *30*, 1923-1933
- (44) Fukui, K. The path of chemical reactions the IRC approach. *Acc. Chem. Res.* **1981**, *14*, 363-368 (45) Groves, J. T.; Adhyam, D. V. Hydroxylation by cytochrome P-450 and metalloporphyrin models. Evidence for allylic rearrangement. *J. Am. Chem. Soc.* **1984**, *106*, 2177-2181
- (46) Newcomb, M.; Shen, R.; Choi, S.-Y.; Toy, P. H.; Hollenberg, P. F.; Vaz, A. D. N.; Coon, M. J. Cytochrome P450-Catalyzed Hydroxylation of Mechanistic Probes that Distinguish between Radicals and Cations. Evidence for Cationic but Not for Radical Intermediates. *J. Am. Chem. Soc.* **2000**, *122*, 2677-2686
- (47) Newcomb, M.; Le Tadic-Biadatti, M.-H.; Chestney, D. L.; Roberts, E. S.; Hollenberg, P. F. A nonsynchronous concerted mechanism for cytochrome P-450 catalyzed hydroxylation. *J. Am. Chem. Soc.* **1995**, *117*, 12085-12091

- (48) Toy, P. H.; Newcomb, M.; Hollenberg, P. F. Hypersensitive Mechanistic Probe Studies of Cytochrome P450-Catalyzed Hydroxylation Reactions. Implications for the Cationic Pathway. *J. Am. Chem. Soc.* **1998**, *120*, 7719-7729
- (49) Yang, B.; Gagliardi, L.; Truhlar, D. G. Transition states of spin-forbidden reactions. *Phys. Chem. Phys.* **2018**, *20*, 4129-4136
- (50) Black, K.; Liu, P.; Xu, L.; Doubleday, C.; Houk, K. N. Dynamics, transition states, and timing of bond formation in Diels-Alder reactions. *Proc. Natl. Acad. Sci. U. S. A.* **2012**, *109*, 12860-12865
- (51) Yang, Z.; Houk, K. N. The Dynamics of Chemical Reactions: Atomistic Visualizations of Organic Reactions, and Homage to van 't Hoff. *Chem. Eur. J.* **2018**, *24*, 3916-3924
- (52) Horn, B. A.; Herek, J. L.; Zewail, A. H. Retro-Diels-Alder Femtosecond Reaction Dynamics. *J. Am. Chem. Soc.* **1996**, *118*, 8755-8756
- (53) Yoshizawa, K.; Kamachi, T.; Shiota, Y. A Theoretical Study of the Dynamic Behavior of Alkane Hydroxylation by a Compound I Model of Cytochrome P450. *J. Am. Chem. Soc.* **2001**, *123*, 9806-9816 (54) Elenewski, J. E.; Hackett, J. C. Ab initio dynamics of the cytochrome P450 hydroxylation reaction. *J. Chem. Phys.* **2015**, *142*, 064307
- (55) Yang, Z.; Yu, P.; Houk, K. N. Molecular Dynamics of Dimethyldioxirane C–H Oxidation. *J. Am. Chem. Soc.* **2016**, *138*, 4237-4242
- (56) Carpenter, B. K. Dynamic Behavior of Organic Reactive Intermediates. *Angew. Chem., Int. Ed.* **1998**, *37*, 3340-3350
- (57) Guo, W.; Hare, S. R.; Chen, S. S.; Saunders, C. M.; Tantillo, D. J. C-H Insertion in Dirhodium Tetracarboxylate-Catalyzed Reactions despite Dynamical Tendencies toward Fragmentation: Implications for Reaction Efficiency and Catalyst Design. *J Am Chem Soc* **2022**, *144*, 17219-17231
- (58) Chen, Z.; Nieves-Quinones, Y.; Waas, J. R.; Singleton, D. A. Isotope Effects, Dynamic Matching, and Solvent Dynamics in a Wittig Reaction. Betaines as Bypassed Intermediates. *J. Am. Chem. Soc.* **2014**, *136*, 13122-13125
- (59) Carpenter, B. K. Dynamic Matching: The Cause of Inversion of Configuration in the [1,3] Sigmatropic Migration? *J. Am. Chem. Soc.* **1995**, *117*, 6336-6344
- (60) Carpenter, B. K. Nonstatistical Dynamics in Thermal Reactions of Polyatomic Molecules. *Annu. Rev. Phys. Chem.* **2004**, *56*, 57-89
- (61) Doubleday, C.; Suhrada, C. P.; Houk, K. N. Dynamics of the Degenerate Rearrangement of Bicyclo[3.1.0]hex-2-ene. *J. Am. Chem. Soc.* **2006**, *128*, 90-94
- (62) Ussing, B. R.; Hang, C.; Singleton, D. A. Dynamic Effects on the Periselectivity, Rate, Isotope Effects, and Mechanism of Cycloadditions of Ketenes with Cyclopentadiene. *J. Am. Chem. Soc.* **2006**, *128*, 7594-7607
- (63) Lourderaj, U.; Hase, W. L. Theoretical and Computational Studies of Non-RRKM Unimolecular Dynamics. *J. Phys. Chem. A* **2009**, *113*, 2236-2253
- (64) Collins, P.; Kramer, Z. C.; Carpenter, B. K.; Ezra, G. S.; Wiggins, S. Nonstatistical dynamics on the caldera. *J. Chem. Phys.* **2014**, *141*, 034111
- (65) Soler, J.; Gergel, S.; Klaus, C.; Hammer, S. C.; Garcia-Borràs, M. Enzymatic Control over Reactive Intermediates Enables Direct Oxidation of Alkenes to Carbonyls by a P450 Iron-Oxo Species. *J. Am. Chem. Soc.* **2022**, *144*, 15954-15968

TOC graphic

